Altered thrombus formation in von Willebrand factor–deficient mice expressing von Willebrand factor variants with defective binding to collagen or GPIIbIIIa

Isabelle Marx,[1,2] Olivier D. Christophe,[1] Peter J. Lenting,[3] Alain Rupin,[2] Marie-Odile Vallez,[2] Tony J. Verbeuren,[2] and Cécile V. Denis[1]

[1]Inserm U770 and Universite Paris-Sud, Le Kremlin-Bicêtre, France; [2]Division of Angiology, Servier Research Institute, Suresnes, France; and [3]Laboratory for Thrombosis and Haemostasis, Department of Clinical Chemistry and Haematology, University Medical Center Utrecht, Utrecht, The Netherlands

The role of von Willebrand factor (VWF) in thrombosis involves its binding to a number of ligands. To investigate the relative importance of these particular interactions in the thrombosis process, we have introduced mutations into murine VWF (mVWF) cDNA inhibiting VWF binding to glycoprotein (Gp) Ib, GPIIbIIIa, or to fibrillar collagen. These VWF mutants were expressed in VWF-deficient mice (VWF$^{-/-}$) by using an hydrodynamic injection approach, and the mice were studied in the ferric chloride–induced injury model. Expression of the collagen and the GPIIbIIIa VWF-binding mutants in VWF$^{-/-}$ mice resulted in delayed thrombus growth and significantly increased vessel occlusion times compared with mice expressing wild-type (WT) mVWF (30 ± 3 minutes and 38 ± 4 minutes for the collagen and GPIIbIIIa mutants, respectively, vs 19 ± 3 minutes for WT mVWF). Interestingly, these mutants were able to correct bleeding time as efficiently as WT mVWF. In contrast, VWF$^{-/-}$ mice expressing the GPIb binding mutant failed to restore thrombus formation and were bleeding for as long as they were observed, confirming the critical importance of the VWF-GPIb interaction. Our observations suggest that targeting the VWF-collagen or VWF-GPIIbIIIa interactions could be an interesting alternative for new antithrombotic strategies. (Blood. 2008;112:603-609)

Introduction

Adhesion and aggregation of platelets at the site of vessel wall injury are critical steps in thrombus formation and subsequent arrest of bleeding. One of the plasma proteins that play a central role in hemostasis and arterial thrombosis is von Willebrand factor (VWF). At high shear stress, VWF establishes the initial tethering of platelets to the injured vessel wall by forming a bridge between platelet receptor glycoprotein (GP) Ib and components of the subendothelium such as collagen.[1] This initial binding step leads to platelet activation and exposition of platelet receptor GPIIbIIIa. The interaction of GPIIbIIIa with fibrinogen and VWF then promotes firm adhesion of platelets to the vessel wall and thrombus growth.

VWF is a multimeric plasma protein produced by endothelial cells and megakaryocytes. It circulates in the plasma at a concentration of 5 to 10 μg/mL, and its subunit is organized in 5 types of repeated domains arranged in the order D′-D3-A1-A2-A3-D4-B1-B2-B3-C1-C2-CK.[2] In vitro approaches have helped identify the functional domains of VWF involved in platelet adhesion and aggregation. The A3 domain plays a predominant role in VWF binding to fibrillar collagen,[3] whereas the A1 domain contains VWF binding site for platelet GPIb.[4] The binding site of VWF for platelet receptor GPIIbIIIa has been located in the C1 domain encompassing the RGD sequence.[5,6] Analysis of patients suffering from von Willebrand disease (VWD), the heterogeneous bleeding disorder resulting from defects in the *VWF* gene, also greatly contributed to the increase in our knowledge about the structure-function relationship of VWF. In particular, molecular variants have proven very useful in establishing the direct link between a specific functional domain and its physiologic relevance.[7]

The critical importance of VWF in thrombus formation has been confirmed in vivo. Indeed, in a ferric chloride–induced arterial thrombosis model, VWF-deficient mice displayed reduced platelet adhesion and thrombus formation.[8,9] However, only complete VWF deficiency was tested in this model. No indication about the relative importance of specific functional domains of VWF in thrombotic events is currently available. To test the physiologic relevance of particular VWF domains in vivo, we previously developed a murine model allowing transient high expression of different VWF mutants in the plasma of VWF$^{-/-}$ mice.[10] Using this model based on hydrodynamic tail vein injection, we have investigated in this study the role of specific VWF mutations in 2 distinct arterial thrombosis models by directly monitoring the process of thrombus growth in live mice.

Methods

Mice

VWF-deficient[8] and wild-type (WT) mice on a C57BL/6 background were used throughout this study. Housing and experiments were done as recommended by French regulations and the experimental guidelines of the European Community.

Submitted February 29, 2008; accepted April 28, 2008. Prepublished online as *Blood* First Edition paper, May 16, 2008; DOI 10.1182/blood-2008-02-142943.

The publication costs of this article were defrayed in part by page charge payment. Therefore, and solely to indicate this fact, this article is hereby marked "advertisement" in accordance with 18 USC section 1734.

Hydrodynamic injection of plasmid DNA

Plasmid DNA diluted in a volume of saline (0.9% NaCl) equivalent to 10% of the bodyweight (ie, 2 mL for a 20 g mouse) was injected into the mouse tail vein within 5 seconds as previously described.[11,12] A 2-mL syringe with a 27-gauge needle was used. No mortality was observed after hydrodynamic injection.

Selection and construction of mVWF mutants

The full-length murine *Vwf* (m*Vwf*) cDNA comprising a Cys at position 799 inserted into the pcDNA6-V5-His expression vector was used.[13] Selection of amino acid residues for mutagenesis on m*Vwf* cDNA and construction of mutants were described in our previous study.[10] Briefly, to inhibit the VWF binding to platelet GPIb, we mutated the Lys residue at position 1362 to Ala (K1362A).[4] The RGD sequence, which is responsible for VWF binding to GPIIbIIIa, was mutated to an RGG sequence by changing residue Asp at position 2509 to Gly (D2509G).[6,14] To abolish VWF binding to collagen, residues Asp 1742, Ser 1783, and His 1786 located in the A3 domain were mutated to Ala (D1742A, S1783A, and H1786A).[3] To obtain prolonged expression of the VWF transgene by the liver, we introduced the full-length WT or mutated m*Vwf* cDNA into the pLIVE expression vector (Mirus Bio, Madison, WI), a vector driven by a liver-specific promoter composed of the minimal mouse albumin promoter and the mouse alpha fetoprotein enhancer II. The pLIVE plasmid was constructed as follows. The full-length cDNA of WT or mutated m*Vwf* inserted into the pcDNA6-V5-His expression vector was amplified by polymerase chain reaction (PCR) with *Asc*I and *Sac*II restriction sites in 5′ and 3′ ends using forward primer 5′-TATAATGGCGCGCCCTC*AACATGG*ACCCTTTCAGGTATGAGA-3′ and reverse primer 5′-GGTGGTCCGCGGGTCTCACTTGCTGCAG-TTCCG-3′. To obtain optimal translation efficiency of m*Vwf* mRNA, we designed the sequence around the ATG start codon (italicized in the forward primer) such that it matches the Kozak translational consensus sequence: ANNATGG. The *Asc*I-*Sac*II fragments of WT or mutated m*Vwf* cDNA were then cloned into the pLIVE vector. To check the absence of undesired mutations, wt m*Vwf* cDNA and the 3 mVWF mutants inserted into the pLIVE vector were entirely sequenced using an ABI PRISM Dye Terminator Cycle Sequencing Reaction Kit v3.1 (Applied Biosystems, Applera, Courtaboeuf, France) on an ABI PRISM 310 DNA sequencer according to the manufacturer's specifications. Plasmid DNA was amplified in *Escherichia coli* DH5α cells and purified by a Nucleobond endotoxin-free plasmid DNA PC 2000 kit (Macherey-Nagel, Hoerdt, France). The purity and quantity of the plasmid DNA were analyzed by agarose gel electrophoresis and by absorbance at 260 and 280 nm.

Blood collection and determination of mVWF levels by enzyme-linked immunosorbent assay

Mice were anesthetized by intraperitoneal injection of sodium pentobarbital (60 mg/kg; Ceva Santé Animale, Libourne, France), and blood was collected from the retroorbital venous plexus into plastic tubes containing trisodium citrate (9 vol blood to 1 vol 0.138 M trisodium citrate). Blood was collected after each hydrodynamic injection of m*Vwf* cDNA at the end of the experiment. To obtain platelet-poor plasma, blood samples were centrifuged at 1000*g* for 20 minutes at room temperature.

Plasma VWF concentration was measured according to a previously described immunosorbent assay[15] using a polyclonal antibody anti–human VWF (Dako, Trappes, France) and a horseradish peroxidase–conjugated polyclonal antibody anti–human VWF (Dako). Normal pooled plasma from 15 C57Bl/6 WT mice was used as a reference and set at 100%. Results were expressed as a percentage of normal murine VWF level.

VWF structure analysis

The multimeric structure of VWF was analyzed by 0.1% sodium dodecyl sulfate (SDS) and 1% agarose (GE Healthcare, Velizy, France) gel electrophoresis.[16] Multimers were visualized using an alkaline phosphatase–conjugated anti–human VWF polyclonal antibody.

Bleeding time

Mouse tail-bleeding time was performed as described previously.[10] Briefly, nonanesthetized mice were placed into a restraining device, and 3 mm of the distal tail was cut using a scalpel. The amputated tail was immersed immediately in physiologic saline at 37°C, and bleeding time was measured from the moment of transection until first arrest of bleeding. Observation was stopped at 600 seconds when bleeding did not cease.

In vivo thrombosis models

Intravital microscopy was performed with a Leica DM LFSA microscope (Leica Microsystèmes SAS, Rueil-Malmaison, France), and images of thrombus formation were captured with a CoolSNAP HQ2 CCD camera (Roper Scientific, Evry, France) alternatively with transmitted and fluorescent light. Thrombi were analyzed using the MetaMorph imaging system (Universal Imaging, Downingtown, PA). To facilitate visualization of thrombus formation, platelets were fluorescently labeled in vivo by injection of DIOC6 (1.25 μM/kg; Sigma-Aldrich, Saint Quentin Fallavier, France)

Laser-induced injury. Laser injury was induced as described by Furie et al[17] with slight modifications. Male mice (5 to 8 weeks old) were anesthetized with an intraperitoneal injection of sodium pentobarbital and were placed on a heating blanket to maintain the body temperature at 37°C. The trachea was intubated to facilitate breathing, and the jugular vein was cannulated for the injection of DIOC6. Injection of DIOC6 was repeated when necessary. The cremaster muscle was then exteriorized and prepared as described by Vicaut et al,[18] and was superfused with preheated saline solution. Arterioles with a diameter of 35 to 60 μm were selected, and localized injury was induced on the vascular endothelium with a diode-pumped crystal Q-switched pulsed laser (440 nm; CrystaLaser, Reno, NV) focused through the microscope objective (40×/0.8 NA water-immersion objective). Multiple upstream injuries were induced within the same animal. To characterize thrombus formation, we defined the following: (1) the kinetic of platelet accumulation; (2) the time required for the thrombus to reach maximal peak size; and (3) maximal surface reached at the peak for each thrombus.

Ferric chloride–induced injury. Ferric chloride injury was induced as described by Denis et al[8] with slight modifications. Male and female mice (3 to 4 weeks old) were anesthetized with an intraperitoneal injection of sodium pentobarbital, and DIOC6 was injected via the tail vein. The mesentery was then exteriorized through a midline abdominal incision, and a single arteriole was selected based on size (100-130 μm) and vessel exposure. A filter paper strip (1/2 × 4 mm) saturated with ferric chloride solution ($FeCl_3$ 10%; Prolabo, Paris, France) was applied on the surface of the arteriole. After 5 minutes of exposure, the filter paper was removed, the preparation was rinsed with preheated physiologic saline, and the platelet accumulation was recorded with a 10×/0.3 NA air objective for 45 minutes from the time of filter paper placement. Time to initial thrombus formation with a diameter greater than 30 μm and time to occlusion were recorded.

Statistical analysis

Data are expressed as mean values plus or minus SEM. Statistical analyses were performed by the Student unpaired *t* test or by one-way analysis of variance (ANOVA). A *P* value less than .05 was considered statistically significant. For ANOVA, in case of *P* less than .05, pairwise comparisons against the control group were made. Corrections for multiple comparisons were made according to Dunnet. Bleeding times and occlusion times that exceeded 600 seconds and 45 minutes were handled as 600 seconds and 45 minutes.

Results

Time course of m*Vwf* gene expression

Due to the transient expression of mVWF obtained in our previous study[10] with the pcDNA6 expression vector (CMV promoter), we

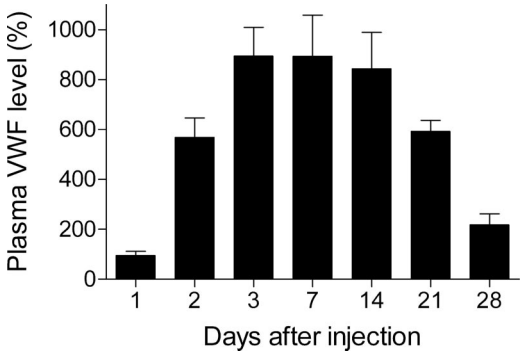

Figure 1. Time-course of mVWF expression after hydrodynamic injection of pLIVE-m*Vwf* in VWF$^{-/-}$ mice. VWF$^{-/-}$ mice (n = 5-9 for each time point) were injected within 5 seconds with a large volume of saline containing 50 μg pLIVE-mVWF. Blood samples were collected at different time points after injection, and plasma mVWF expression was determined by enzyme-linked immunosorbent assay. Data are presented as means plus or minus SEM.

have introduced m*Vwf* cDNA into the pLIVE expression vector (pLIVE-mVWF), a vector driven by a liver-specific promoter and described as leading to sustained expression of the transgene.

To test the ability of pLIVE-m*Vwf* to mediate long-term gene transfer, we injected 50 μg pLIVE-m*Vwf* in VWF$^{-/-}$ mice, and blood was collected 1, 2, 3, 7, 14, 21, and 28 days after injection. Hydrodynamic gene transfer resulted in very high expression of mVWF antigen, and peak plasma VWF level was reached 3 days after gene transfer with a mVWF mean expression of 893% (± 115%; Figure 1). Murine VWF expression levels were sustained for 2 weeks and then decreased gradually. At 4 weeks after gene transfer, mVWF levels were still 2 times higher than in WT mice. Furthermore, we observed that mVWF expression levels were similar in male and in female mice in contrast to pcDNA6 expression vector, which resulted in expression of mVWF twice as important in males than in females.[10]

Based on these results, we have introduced m*Vwf* cDNA mutated in the RGD sequence (D2509G), in the collagen-binding site (D1742A, S1783A, H1786A), or in the GPIb-binding site (K1362A) into the pLIVE expression vector. VWF$^{-/-}$ mice injected with 50 μg of mutated m*Vwf* cDNA resulted in plasma VWF antigen levels similar to those obtained with WT m*Vwf* cDNA 3 to 4 days after injection. Indeed, expression of the RGG mutant amounted to 99.7% of expression obtained with WT m*Vwf* ($P = .68$), whereas expression of the collagen mutant and the GPIb mutant amounted to 84.05% and 75.7% of WT, respectively ($P = .85$ and $P = .5$). Furthermore, the multimeric pattern of mutated mVWF was comparable with the pattern seen in VWF$^{-/-}$ mice injected with WT m*Vwf* cDNA (Figure 2).

Effect of WT and mutated mVWF on bleeding time

To assess whether hydrodynamic injection of pLIVE-m*Vwf* could correct the bleeding time in VWF$^{-/-}$ mice, we injected 50 μg of WT or mutated m*Vwf* cDNA into VWF$^{-/-}$ mice. Bleeding time was determined by transection of the tail tip 3 days after injection. As shown in Figure 3, WT mice stopped bleeding in less than 100 seconds, whereas noninjected VWF$^{-/-}$ mice bled for the entire observation period (> 600 seconds). VWF$^{-/-}$ mice injected with WT m*Vwf* cDNA significantly corrected bleeding time 3 days after injection ($P < .001$ compared with noninjected VWF$^{-/-}$ mice). Injection of a pLIVE empty vector did not change the bleeding time of VWF$^{-/-}$ mice. After injection of m*Vwf* cDNA, bleeding time in VWF-deficient mice was no longer different from bleeding time in WT mice (100 ± 18 seconds vs 79 ± 4 seconds; $P = .33$). Injection of the collagen-binding mutant and

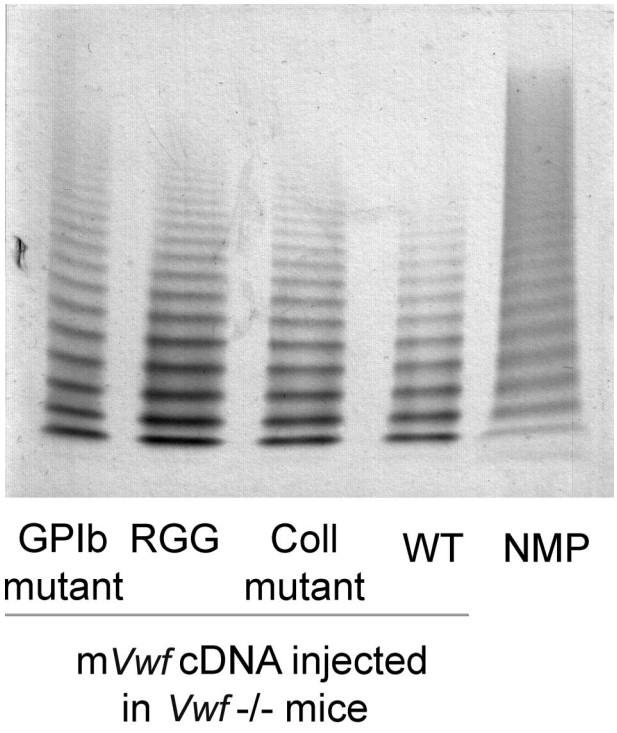

Figure 2. Multimeric composition of plasma mVWF after hydrodynamic gene delivery. VWF$^{-/-}$ mice were injected with 50 μg of WT pLIVE-m*Vwf* (WT) or pLIVE-m*Vwf* mutated in the RGD sequence (RGG), in the collagen-binding site (Coll mutant), or in the GPIb-binding site (GPIb mutant). Plasma was collected 72 hours later, and analysis of plasma samples was performed by SDS/1% agarose gel electrophoresis. NMP indicates normal mouse plasma.

RGG mutant in VWF$^{-/-}$ mice also resulted in a complete correction of bleeding time, with values of 83 plus or minus 9 seconds, and 106 plus or minus 21 seconds, respectively, similar to the correction obtained with injection of WT m*Vwf* cDNA. In contrast, mice injected with the GPIb binding mutant were bleeding during the 600-second observation period. Injection of pLIVE vector in WT mice did not significantly affect bleeding time.

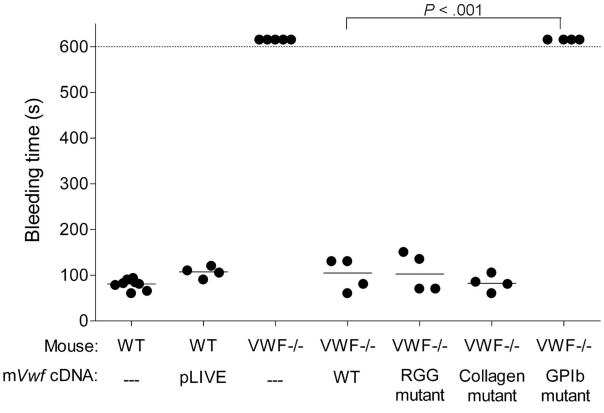

Figure 3. Effect of WT and mutated mVWF on bleeding time in VWF$^{-/-}$ mice after hydrodynamic gene delivery. VWF$^{-/-}$ mice were injected with 50 μg of WT pLIVE-m*Vwf* or pLIVE-m*Vwf* mutated in the RGD sequence (D2509G), in the collagen-binding site (D1742A, S1783A, H1786A), or in the GPIb-binding site (K1362A). Bleeding time was assessed 3 days after injection by tail tip transection. Observation was stopped at 600 seconds when bleeding did not cease. Each symbol represents one mouse, and the median value of each group is represented by a horizontal line. pLIVE stands for mice injected with the vector only. NS indicates not significant.

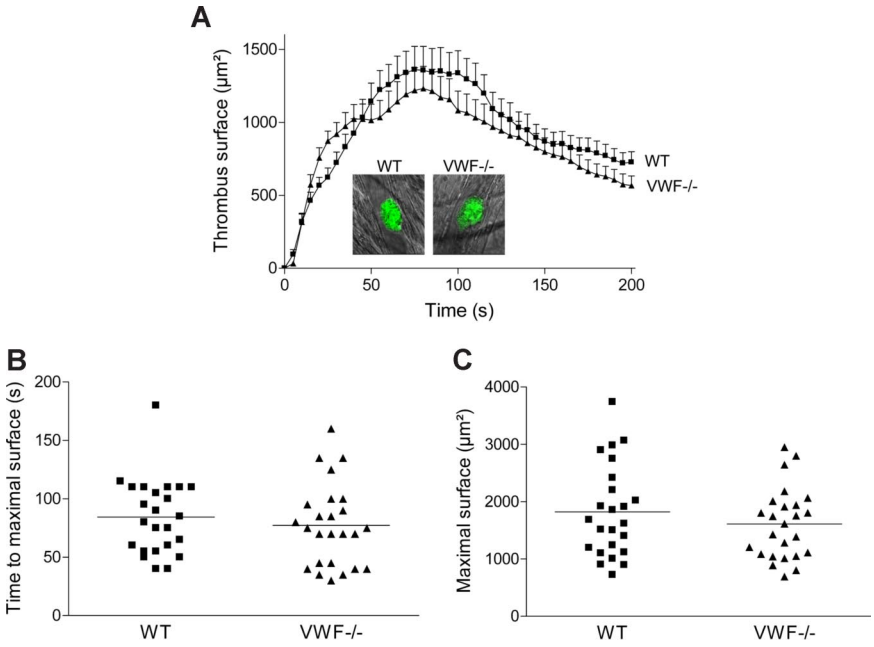

Figure 4. Thrombus formation after laser-induced injury in cremaster arterioles of WT and VWF$^{-/-}$ mice. Localized laser injury was induced to endothelial cells of arterioles with a diameter of 35 to 60 μm, and thrombus growth was immediately recorded (1-second intervals). (A) The mean thrombus surface versus time after laser-induced injury (24 thrombi in 6 WT mice and 25 thrombi in 5 VWF$^{-/-}$ mice). The mean thrombus surface was analyzed every 5 seconds; data are presented as means plus or minus SEM. The photographs represent the thrombus at maximal size in a WT and a VWF$^{-/-}$ mouse after laser injury. Original magnification, ×400. (B) Time required for maximal surface for each thrombus in WT and VWF$^{-/-}$ mice. The mean time of each group is indicated by a horizontal line, and no significant difference was observed ($P = .46$). (C) Maximal surface reached at the peak for each thrombus in WT and VWF$^{-/-}$ mice. The mean maximal surface of each group is indicated by a line, and no significant difference was observed ($P = .31$).

Thrombus formation in WT and VWF$^{-/-}$ mice using a laser-induced injury thrombosis model

To examine in vivo the role of specific VWF mutations on thrombus formation, we first investigated whether platelet adhesion and aggregation were altered in VWF$^{-/-}$ mice in a cremaster arteriole thrombosis model. Localized laser injury was induced to the luminal vessel surface, and thrombus development was immediately recorded for up to 200 seconds. A total of 24 thrombi in 6 WT mice and 25 thrombi in 5 VWF$^{-/-}$ mice were generated. In WT mice, platelets adhered and accumulated rapidly at the site of injury, and platelet accumulation reached maximal surface at approximately 80 seconds after injury (Figure 4). The thrombus then decreased in size and stabilized in approximately 3 minutes after injury. In VWF$^{-/-}$ mice, the kinetic of thrombus formation was similar to that of WT mice with no difference in thrombus size. The mean time required for maximal thrombus size and the mean maximal surface reached at the peak for each thrombus were comparable in WT and VWF$^{-/-}$ mice (84 ± 7 seconds vs 77 ± 7 seconds; $P = .46$ and 1821 ± 164 μm^2 vs 1610 ± 124 μm^2; $P = .31$, respectively). These results indicate that platelet adhesion and aggregation are not dependent on VWF after laser-induced injury in the cremaster microcirculation. Because there was no major difference in thrombus formation between VWF$^{-/-}$ and WT mice, we concluded that this particular thrombosis model was not appropriate to test the different VWF mutants.

$FeCl_3$-induced injury thrombosis model

Thrombus formation was impaired in VWF$^{-/-}$ mice. We next examined the role of VWF in platelet adhesion and aggregation after applying 10% $FeCl_3$ for 5 minutes to the external vessel wall surface. Ferric chloride induces the formation of reactive oxygen species, leading to endothelial denudation and exposure of subendothelial matrix components to flowing blood. Platelet accumulation in mesenteric vessels of 100 to 130 μm in diameter was recorded for 45 minutes, and images were taken every minute. In WT mice, after removing the $FeCl_3$ filter paper, platelets adhered to the injured vessel wall and started to form visible platelet aggregates a few minutes later (Figure 5). As shown in Figure 6, the median time required for formation of an initial thrombus greater than 30 μm in diameter was 7.6 plus or minus 0.6 minutes. Subsequently, thrombi grew fast and occluded the vessel at the site of injury after approximately 20 minutes. In VWF$^{-/-}$ mice, the formation of first aggregates was significantly delayed, and the median time for initial thrombus formation was more than twice as long as in WT mice (Figure 6). In addition, in these mice, thrombi grew very slowly, and none of the vessels occluded during the 45-minute observation period (Figure 5). At 45 minutes, we only observed the presence of several small thrombi. These results indicate that VWF plays a critical role in platelet accumulation and thrombus formation after a $FeCl_3$-induced vessel wall injury.

Thrombus formation was restored in VWF$^{-/-}$ mice after hydrodynamic injection of WT mVwf cDNA. We next evaluated whether hydrodynamic gene transfer of 50 μg of m*Vwf* cDNA could correct thrombus formation in VWF$^{-/-}$ mice. A $FeCl_3$ thrombosis model was induced 3 to 4 days after injection of m*Vwf* cDNA. As shown in Figure 5, administration of m*Vwf* cDNA in VWF$^{-/-}$ mice resulted in complete restoration of thrombus formation. The time course of thrombus formation and thrombus size were comparable in injected VWF$^{-/-}$ mice and WT mice. There were no significant differences in the median time for initial thrombus formation ($P = .28$) and in the median time for the formation of an occlusive thrombus ($P = .85$) between injected VWF$^{-/-}$ mice and WT mice (Figure 6).

Thrombus formation was altered in VWF$^{-/-}$ mice after hydrodynamic injection of mutated mVwf cDNA. To examine the role of specific functional domains of VWF in platelet accumulation and thrombus formation, we transfected VWF$^{-/-}$ mice with 50 μg of m*Vwf* cDNA mutated in the RGD sequence (D2509G), in the collagen-binding site (D1742A, S1783A, H1786A), or in the GPIb-binding site (K1362A). After hydrodynamic injection of collagen-binding mutant and RGG mutant in VWF$^{-/-}$ mice, the time required for formation of an initial thrombus greater than 30 μm in diameter was similar to the time obtained with injection of WT m*Vwf* cDNA, with values of 9.3 ($\pm$ 0.9) minutes and 8.0 ($\pm$ 0.7) minutes, respectively (Figure 6). In these mice, however, thrombus growth was significantly delayed compared

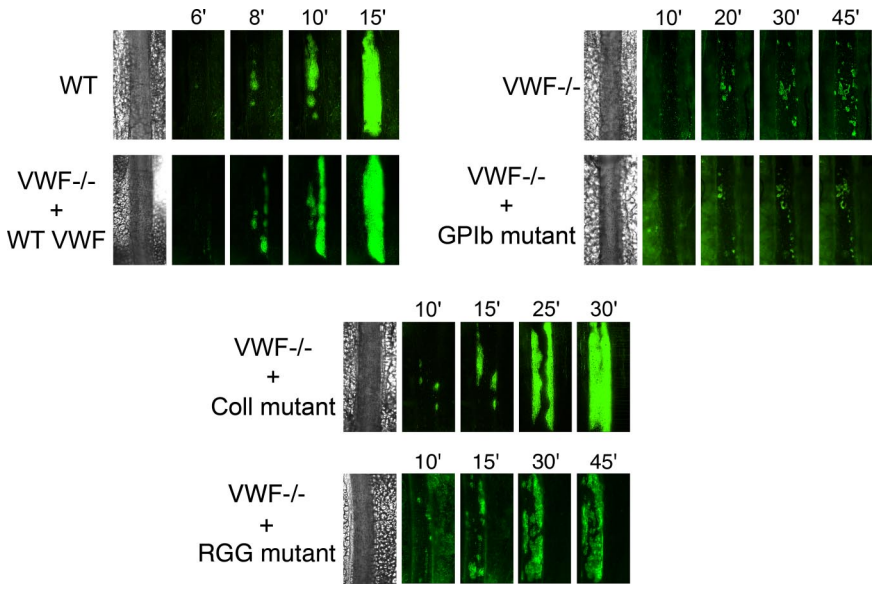

Figure 5. Representative images of thrombus growth versus time after ferric chloride–induced injury. Thrombus formation was induced with 10% $FeCl_3$ for 5 minutes in mesenteric arterioles, and platelet accumulation was analyzed for 45 minutes from the time of filter paper placement. Images of thrombus growth were taken every minute alternatively in transmitted and fluorescent light. $VWF^{-/-}$ mice were injected with 50 μg of WT m*Vwf* cDNA and m*Vwf* cDNA mutated in the RGD sequence (D2509G), in the collagen-binding site (D1742A, S1783A, H1786A), or in the GPIb-binding site (K1362A). Original magnification, ×100.

with $VWF^{-/-}$ mice injected with WT m*Vwf* cDNA (Figure 5). Indeed, injection of the collagen-binding mutant in $VWF^{-/-}$ mice resulted in occlusive thrombi at 30.1 (± 2.8) minutes, 10 minutes later than in $VWF^{-/-}$ mice injected with WT cDNA. Regarding $VWF^{-/-}$ mice injected with the RGG mutant, only 3 mice of 8 reached occlusion of the arteriole within 45 minutes. In these mice, we could observe the formation of thrombi that seemed to occupy the entire lumen of the vessel, but these thrombi were less compact than those obtained in WT m*Vwf* cDNA–injected mice, and they could not stop blood flow. In addition, there was continuous embolization of small parts of the thrombus, explaining the delayed or absent occlusion in these mice.

Finally, $VWF^{-/-}$ mice injected with the GPIb-binding mutant did not restore thrombus formation and presented a course of platelet accumulation similar to noninjected $VWF^{-/-}$ mice. The median time for initial thrombus formation was 23.0 (± 3.1) minutes, and arterioles did not occlude during the observation period.

Discussion

VWF plays an important role in arterial thrombosis as demonstrated by the defective thrombus formation observed in $VWF^{-/-}$ mice.[8] The mechanism underlying VWF implication in the thrombotic process is complex and involves its interaction with different ligands, the subendothelial collagens, GPIb, and GPIIbIIIa. The relative importance of these different interactions is unclear because, as of yet, only the complete absence of VWF has been evaluated in in vivo thrombosis models. In the present study, we have measured the thrombotic response of mice expressing VWF variants presenting defective binding to either collagen, GPIb or GPIIbIIIa. To express these various VWF derivatives, we have used the hydrodynamic injection approach allowing transient expression of high levels of plasma VWF. We have previously validated this technique using WT m*Vwf* cDNA which, after injection in VWF-deficient mice, led to a correction of bleeding symptoms.[10] In contrast to our previous study in which m*Vwf* cDNA was subcloned in the pcDNA6 expression vector, leading to short-term expression of the protein, we have now ligated m*Vwf* cDNA into the pLIVE expression vector, a vector expressly designed for hydrodynamic injection with a liver-specific promoter. After injection of this construct in $VWF^{-/-}$ mice, we observed long-lasting and very high mVWF plasma antigen levels. The antigen peak was reached 3 days after injection and was sustained for 14 days. The slow decline in expression levels after 2 weeks appears to be the result of an immune response directed against the expressed protein.[19]

Because thrombus formation is dependent on the type and severity of the vascular injury and on the vascular bed targeted, we compared 2 distinct arterial models of thrombosis in $VWF^{-/-}$ mice, one initiated by a localized laser-induced injury in the cremaster microcirculation and the other one initiated by denudation of the endothelium by $FeCl_3$ in the mesenteric microcirculation. Surprisingly, in the laser-induced thrombosis model, $VWF^{-/-}$ mice displayed a thrombotic response similar to WT mice. In agreement with our results, Dubois et al reported only a slight reduction in the maximal size of $VWF^{-/-}$ thrombi compared with WT thrombi in a similar laser-induced thrombosis model of cremaster arterioles.[20] One likely explanation for the VWF-independent platelet aggregation and thrombus growths after laser-induced injury is the strong dependency of this model to thrombin. Indeed, high levels of thrombus-associated tissue factor (TF) could be detected in this model, and several studies have shown that treatment with a thrombin inhibitor markedly decreased platelet accumulation after laser injury.[20-22] In addition, it has been shown by in vitro studies that thrombin-induced platelet aggregation is normal in mice lacking VWF.[23,24] A possible explanation to our results thus relates to the capacity of thrombin to overcome the thrombosis defect associated with VWF deficiency in the laser injury thrombosis model, a model dominated by TF-mediated thrombin generation.[25] This model may be more relevant for pathologic thrombus formation in specific conditions such as inflammation, trauma, or bacterial infection.

In contrast to the laser thrombosis model, the $FeCl_3$-induced vessel wall injury is dominated by subendothelial collagen exposure.[21] In this model, consistent with previous findings, $VWF^{-/-}$ mice displayed delayed platelet adhesion and reduced thrombus formation.[8,9] We observed the presence only of small thrombi, and none of the vessels occluded in these mice. Expression of WT mVWF in $VWF^{-/-}$ mice completely restored thrombus formation after vascular injury. Furthermore, we observed complete correction of bleeding time in these mice. Thus, plasma VWF appears to

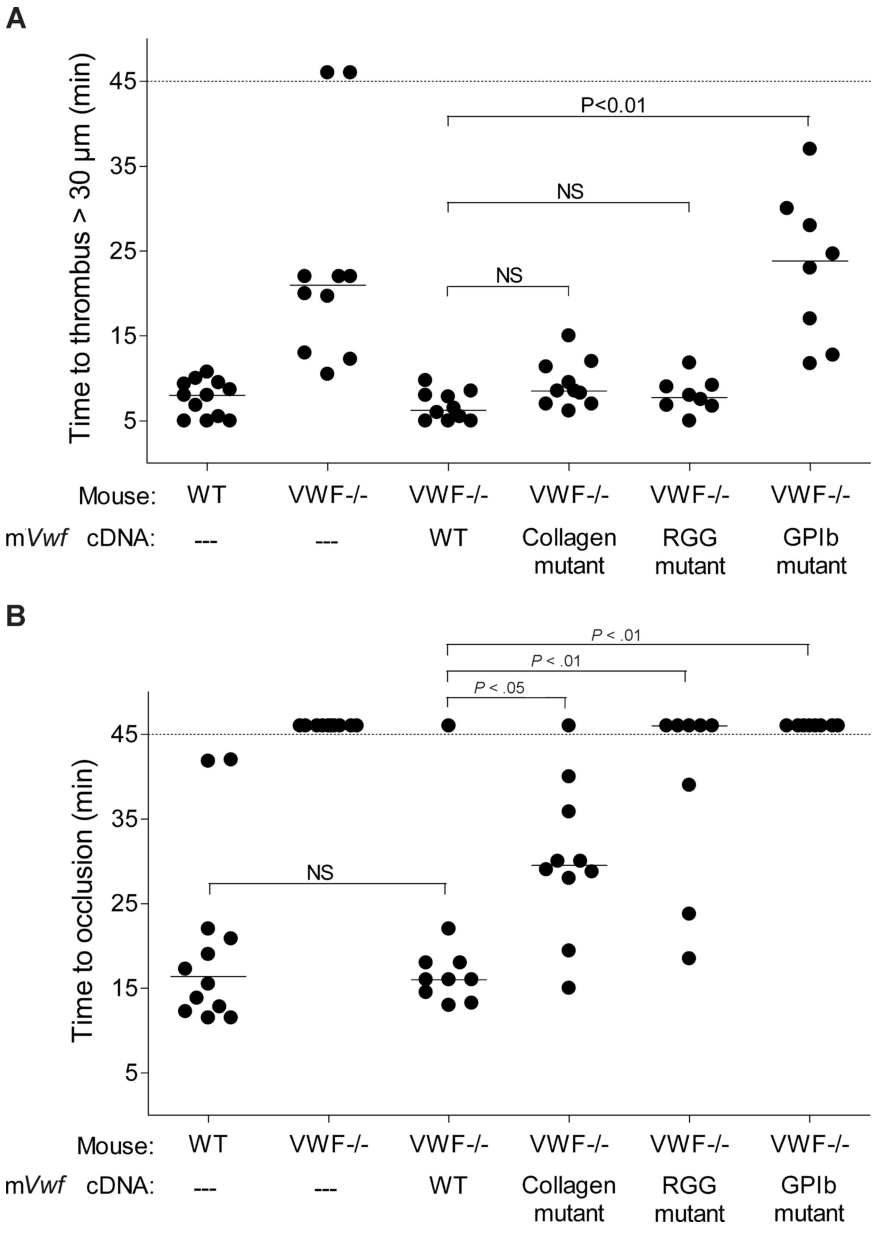

Figure 6. Effect of WT and mutated mVWF on ferric chloride–induced injury in mesenteric arterioles of VWF$^{-/-}$ mice after hydrodynamic injection. VWF$^{-/-}$ mice were injected with 50 μg of WT pLIVE-m*Vwf* or pLIVE-m*Vwf* mutated in the RGD sequence (D2509G), in the collagen-binding site (D1742A, S1783A, H1786A), or in the GPIb-binding site (K1362A). Thrombus formation was examined 3 to 4 days after injection. Endothelial injury was induced with 10% $FeCl_3$ in mesenteric vessels 100 to 130 μm in diameter. When the vessel did not occlude within 45 minutes, observation was stopped. Each symbol represents one mouse, and the median value of each group is indicated. (A) Time required for the formation of the first thrombus greater than 30 μm in diameter. (B) Time required for the formation of an occlusive thrombus (cessation of blood flow).

be sufficient to support efficient thrombosis and hemostasis in VWF$^{-/-}$ mice because VWF is lacking in platelets and endothelial cells after hydrodynamic injection.[10] Restoration of the platelet VWF compartment does not appear necessary for correction of bleeding tendency in VWF$^{-/-}$ mice. These results are in agreement with crossed bone marrow transplantation experiments performed in the porcine model of VWD. Indeed, in VWD pigs that underwent transplantion with bone marrow from normal pigs, only partial or no correction of bleeding time could be observed.[26,27] In addition, in normal pigs grafted with bone marrow from VWD pigs, bleeding time remained unchanged, suggesting only a minimal contribution of platelet VWF in hemostasis.[28]

We next compared the ability of WT and mutant VWF to form platelet thrombi in VWF$^{-/-}$ mice in the $FeCl_3$ injury model in mesenteric arterioles. The total absence of binding of the different VWF mutants to their respective ligands in vitro has been previously verified.[10]

The critical importance of the VWF-GPIb interaction in the first step of platelet adhesion was confirmed with the GPIb-binding mutant, which failed to restore thrombus formation. Mice expressing this mutant presented a course of platelet accumulation similar to noninjected VWF$^{-/-}$ mice. In addition, mice injected with this mutant were bleeding for as long as they were observed. These results are consistent with the observations that agents interfering with the VWF-GPIb axis have previously demonstrated their efficacy as antithrombotic tools in animal models.[29-32]

For the collagen-binding mutant, we mutated residues in the A3 domain identified as being critical for binding to collagen types I and III.[3] VWF$^{-/-}$ mice expressing this mutant exhibited significantly delayed vessel occlusion compared with mice expressing WT mVWF. Although, the occlusion time was greatly delayed in these mice, the thrombi that formed were stable and well anchored to the vessel wall. This result indicates that VWF binding to fibrillar collagen is important in vivo for efficient platelet adhesion to the vessel wall in the $FeCl_3$ injury thrombosis model. Interestingly, this mutant was able to correct bleeding time in VWF$^{-/-}$ mice as efficiently as WT mVWF. Our observations are consistent with a previous study reporting that specific disruption of the

VWF-collagen interaction by a monoclonal antibody against the VWF A3 domain led to reduced thrombus growth in vivo with only slightly prolonged bleeding time.[33]

More surprisingly, mutation of the VWF RGD sequence into RGG also resulted in delayed vessel occlusion, with most arterioles remaining nonocclusive. Bridging bonds between platelets are thus impaired in $VWF^{-/-}$ mice expressing this mutant. Indeed, we observed thrombi that were less compact with constant detaching of small platelet clumps, demonstrating the need for the VWF-GPIIbIIIa interaction in platelet-platelet firm adhesion at high shear rate. Despite the presence of nonocclusive platelet clots in the thrombosis model, this mutant was able to correct bleeding time as efficiently as WT VWF.

In conclusion, our model leads to sustained expression of VWF variants in the plasma of $VWF^{-/-}$ mice, allowing examination of their in vivo function, particularly in thrombosis. Using this approach, we demonstrate here that inhibition of VWF binding to collagen or GPIIbIIIa results in reduced platelet thrombus formation without significant impact on bleeding time. Our results suggest for the first time that inhibition of the VWF-GPIIbIIIa interaction may represent a safer alternative compared with inhibition of GPIIbIIIa, because thrombosis at high shear would be preferentially targeted. These observations make these axes interesting for new antithrombotic strategies.

Authorship

Contributions: I.M. performed experiments and wrote the manuscript; O.C. and A.R. designed the study, analyzed data, and approved the final manuscript; P.J.L. contributed an essential reagent and approved the final manuscript; M.O.V. performed experiments and approved the final manuscript; T.J.V. designed the study and approved the final manuscript; and C.V.D. designed the study, analyzed data, and wrote the manuscript.

Conflict-of-interest disclosure: The authors declare no competing financial interests.

Correspondence: Cécile V. Denis, Inserm U. 770, 80 rue du Général Leclerc, 94276 Le Kremlin-Bicêtre Cedex, France; e-mail: cecile.denis@inserm.fr.

References

1. Ruggeri ZM. Von Willebrand factor. Curr Opin Hematol. 2003;10:142-149.
2. Sadler JE. Biochemistry and genetics of von Willebrand factor. Annu Rev Biochem. 1998;67:395-424.
3. Romijn RA, Westein E, Bouma B, et al. Mapping the collagen-binding site in the von Willebrand factor-A3 domain. J Biol Chem. 2003;278:15035-15039.
4. Matsushita T, Meyer D, Sadler JE. Localization of von Willebrand factor-binding sites for platelet glycoprotein Ib and botrocetin by charged-to-alanine scanning mutagenesis. J Biol Chem. 2000;275:11044-11049.
5. Beacham DA, Wise RJ, Turci SM, Handin RI. Selective inactivation of the Arg-Gly-Asp-Ser (RGDS) binding site in von Willebrand factor by site-directed mutagenesis. J Biol Chem. 1992; 267:3409-3415.
6. Lankhof H, Wu YP, Vink T, et al. Role of the glycoprotein Ib-binding A1 repeat and the RGD sequence in platelet adhesion to human recombinant von Willebrand factor. Blood. 1995;86:1035-1042.
7. Sadler JE, Budde U, Eikenboom JC, et al. Update on the pathophysiology and classification of von Willebrand disease: a report of the Subcommittee on von Willebrand Factor. J Thromb Haemost. 2006;4:2103-2114.
8. Denis C, Methia N, Frenette PS, et al. A mouse model of severe von Willebrand disease: defects in hemostasis and thrombosis. Proc Natl Acad Sci U S A. 1998;95:9524-9529.
9. Ni H, Denis CV, Subbarao S, et al. Persistence of platelet thrombus formation in arterioles of mice lacking both von Willebrand factor and fibrinogen. J Clin Invest. 2000;106:385-392.
10. Marx I, Lenting PJ, Adler T, Pendu R, Christophe OD, Denis CV. Correction of bleeding symptoms in von Willebrand factor-deficient mice by liver-expressed von Willebrand factor mutants. Arterioscler Thromb Vasc Biol. 2008;28:419-424.
11. Liu F, Song Y, Liu D. Hydrodynamics-based transfection in animals by systemic administration of plasmid DNA. Gene Ther. 1999;6:1258-1266.
12. Zhang G, Budker V, Wolff JA. High levels of foreign gene expression in hepatocytes after tail vein injections of naked plasmid DNA. Hum Gene Ther. 1999;10:1735-1737.
13. Lenting PJ, de Groot PG, De Meyer SF, et al. Correction of the bleeding time in von Willebrand factor (VWF)-deficient mice using murine VWF. Blood. 2007;109:2267-2268.
14. Jumilly AL, Veyradier A, Ribba AS, Meyer D, Girma JP. Selective inactivation of Von Willebrand factor binding to glycoprotein IIb/IIIa and to inhibitor monoclonal antibody 9 by site-directed mutagenesis. Hematol J. 2001;2:180-187.
15. Lenting PJ, Westein E, Terraube V, et al. An experimental model to study the in vivo survival of von Willebrand factor. Basic aspects and application to the R1205H mutation. J Biol Chem. 2004; 279:12102-12109.
16. Obert B, Tout H, Veyradier A, Fressinaud E, Meyer D, Girma JP. Estimation of the von Willebrand factor-cleaving protease in plasma using monoclonal antibodies to vWF. Thromb Haemost. 1999;82:1382-1385.
17. Falati S, Gross P, Merrill-Skoloff G, Furie BC, Furie B. Real-time in vivo imaging of platelets, tissue factor and fibrin during arterial thrombus formation in the mouse. Nat Med. 2002;8:1175-1181.
18. Vicaut E, Montalescot G, Hou X, Stucker O, Teisseire B. Arteriolar vasoconstriction and tachyphylaxis with intraarterial angiotensin II. Microvasc Res. 1989;37:28-41.
19. Ye P, Thompson AR, Sarkar R, et al. Naked DNA transfer of Factor VIII induced transgene-specific, species-independent immune response in hemophilia A mice. Mol Ther. 2004;10:117-126.
20. Dubois C, Panicot-Dubois L, Gainor JF, Furie BC, Furie B. Thrombin-initiated platelet activation in vivo is vWF independent during thrombus formation in a laser injury model. J Clin Invest. 2007; 117:953-960.
21. Dubois C, Panicot-Dubois L, Merrill-Skoloff G, Furie B, Furie BC. Glycoprotein VI-dependent and -independent pathways of thrombus formation in vivo. Blood. 2006;107:3902-3906.
22. Nonne C, Lenain N, Hechler B, et al. Importance of platelet phospholipase Cgamma2 signaling in arterial thrombosis as a function of lesion severity. Arterioscler Thromb Vasc Biol. 2005;25:1293-1298.
23. Reheman A, Gross P, Yang H, et al. Vitronectin stabilizes thrombi and vessel occlusion but plays a dual role in platelet aggregation. J Thromb Haemost. 2005;3:875-883.
24. Yang H, Reheman A, Chen P, et al. Fibrinogen and von Willebrand factor-independent platelet aggregation in vitro and in vivo. J Thromb Haemost. 2006;4:2230-2237.
25. Furie B, Furie BC. Thrombus formation in vivo. J Clin Invest. 2005;115:3355-3362.
26. Bowie EJ, Solberg LA, Jr., Fass DN, et al. Transplantation of normal bone marrow into a pig with severe von Willebrand's disease. J Clin Invest. 1986;78:26-30.
27. Nichols TC, Samama CM, Bellinger DA, et al. Function of von Willebrand factor after crossed bone marrow transplantation between normal and von Willebrand disease pigs: effect on arterial thrombosis in chimeras. Proc Natl Acad Sci U S A. 1995;92:2455-2459.
28. Roussi J, Samama M, Vaiman M, et al. An experimental model for testing von Willebrand factor function: successful SLA-matched crossed bone marrow transplantations between normal and von Willebrand pigs. Exp Hematol. 1996;24:585-591.
29. Cauwenberghs N, Meiring M, Vauterin S, et al. Antithrombotic effect of platelet glycoprotein Ib-blocking monoclonal antibody Fab fragments in nonhuman primates. Arterioscler Thromb Vasc Biol. 2000;20:1347-1353.
30. Golino P, Ragni M, Cirillo P, et al. Aurintricarboxylic acid reduces platelet deposition in stenosed and endothelially injured rabbit carotid arteries more effectively than other antiplatelet interventions. Thromb Haemost. 1995;74:974-979.
31. McGhie AI, McNatt J, Ezov N, et al. Abolition of cyclic flow variations in stenosed, endothelium-injured coronary arteries in nonhuman primates with a peptide fragment (VCL) derived from human plasma von Willebrand factor-glycoprotein Ib binding domain. Circulation. 1994;90:2976-2981.
32. Yamamoto H, Vreys I, Stassen JM, Yoshimoto R, Vermylen J, Hoylaerts MF. Antagonism of vWF inhibits both injury induced arterial and venous thrombosis in the hamster. Thromb Haemost. 1998;79:202-210.
33. Wu D, Vanhoorelbeke K, Cauwenberghs N, et al. Inhibition of the von Willebrand (VWF)-collagen interaction by an antihuman VWF monoclonal antibody results in abolition of in vivo arterial platelet thrombus formation in baboons. Blood. 2002;99:3623-3628.